



Published in final edited form as:

Radiother Oncol. 2016 May ; 119(2): 259–264. doi:10.1016/j.radonc.2016.03.027.

Effects of local irradiation combined with sunitinib on early remodeling, mitochondria, and oxidative stress in the rat heart

Vijayalakshmi Sridharan¹, Chanice J. Thomas², Maohua Cao¹, Stepan B. Melnyk³, Oleksandra Pavliv³, Jacob Joseph^{4,5}, Sharda P. Singh⁶, Sunil Sharma⁷, Eduardo G. Moros⁸, and Marjan Boerma¹

¹University of Arkansas for Medical Sciences, Department of Pharmaceutical Sciences, Division of Radiation Health, Little Rock, Arkansas

²Oakwood University, Huntsville, Alabama

³University of Arkansas for Medical Sciences, Department of Pediatrics, Little Rock, Arkansas

⁴Veterans Affairs Boston Healthcare System, Department of Medicine, West Roxbury, Massachusetts

⁵Brigham and Women's Hospital, Department of Medicine, Harvard Medical School, Boston, Massachusetts

⁶University of Arkansas for Medical Sciences, Department of Pharmacology and Toxicology, Little Rock, Arkansas

⁷University of Arkansas for Medical Sciences, Department of Radiation Oncology, Little Rock, Arkansas

⁸Moffitt Cancer Center and Research Institute, Department of Radiation Oncology, Tampa, Florida

Abstract

Background and Purpose—Thoracic (chemo)radiation therapy is increasingly administered with tyrosine kinase inhibitors (TKI). While TKI have adverse effects on the heart, it is unknown whether combination with other cancer therapies causes enhanced toxicity. We used an animal model to investigate whether radiation and sunitinib interact in their effects on the heart.

Material and Methods—Male Sprague-Dawley rats received local heart irradiation (9 Gy per day, 5 days). Oral sunitinib (8 or 15 mg/kg bodyweight per day) started on day 1 of irradiation and continued for 2 weeks. Cardiac function was examined with echocardiography. Cardiac remodeling, cell death, left ventricular (LV) oxidative stress markers, mitochondrial morphology and membrane permeability transition pore (mPTP) opening were assessed.

Correspondence: Marjan Boerma, PhD, University of Arkansas for Medical Sciences, Division of Radiation Health, 4301 West Markham, Slot 522-10, Little Rock AR 72205 Phone: +1-501-686-6599, mboerma@uams.edu.

Conflict of Interest Statement

The authors have no conflicts of interest to declare.

Publisher's Disclaimer: This is a PDF file of an unedited manuscript that has been accepted for publication. As a service to our customers we are providing this early version of the manuscript. The manuscript will undergo copyediting, typesetting, and review of the resulting proof before it is published in its final citable form. Please note that during the production process errors may be discovered which could affect the content, and all legal disclaimers that apply to the journal pertain.

Results—Cardiac diameter, stroke volume, and LV volume, mass and anterior wall thickness increased in time, but only in the vehicle group. Sunitinib reduced LV inner diameter and volume in systole, which were counteracted by radiation. Sunitinib and radiation showed enhanced effects on mitochondrial morphology and mPTP opening, but not on cardiac troponin I, mast cell numbers or markers of oxidative stress.

Conclusions—This study found no early enhanced effects of radiation and sunitinib on cardiac function or structure. Long-term effects remain to be determined.

Keywords

Heart; Ionizing radiation; Sunitinib; Oxidative stress; Mitochondria

Introduction

Long-term survivors of thoracic cancers whose heart was exposed during radiation therapy, may present with cardiac side effects such as conduction abnormalities, accelerated atherosclerosis, myocardial and pericardial fibrosis and injury to cardiac valves [1–3]. Radiation therapy has undergone many improvements in treatment planning and radiation delivery. Nonetheless, a significant subset of patients with thoracic cancers, including those of the lung, esophagus, and proximal stomach, still receive considerable doses of radiation to the heart [4–6].

Tyrosine kinase inhibitors (TKI) have emerged as a new class of targeted cancer treatments. By inhibiting tyrosine kinases, these agents target pathways involved in tumor angiogenesis, proliferation, and metastasis [7]. Several TKIs have been approved or are in clinical development for the treatment of thoracic cancers (e.g., breast, esophagus, and lung) [8–11] and metastatic cancers [12–15]. TKIs are commonly administered concurrently with (chemo)radiation therapy, and continuous dosing of the TKI follows for several months to years afterward. Unfortunately, TKI have shown cardiac side effects in about 1% to 30% of patients [16–18]. Since radiation and several common chemotherapeutic agents have their own adverse effects on the heart, there is a concern about potential additive or synergistic cardiac toxicity of these treatments [19;20]. Here, we start to investigate potential interactions by examining the early effects of TKI in combination with radiation in a preclinical animal model.

Sunitinib malate is an orally active inhibitor of multiple receptor tyrosine kinases [21]. Because of its broad targeting, sunitinib is an effective anti-cancer agent, but it also carries a possibility of side effects that may result from inhibition of off-target kinases. Sunitinib is currently in use for the treatment of several solid tumors, including gastrointestinal stromal tumors, and is tested in clinical trials for breast cancer and non–small cell lung cancer [9;10;13]. Since the cardiotoxic effects of sunitinib have been studied in previous animal models [22–24] that may provide results for comparison, we selected sunitinib as our model TKI.

Materials and Methods

Animal model and local heart irradiation

All procedures were approved by the Institutional Animal Care and Use Committee of the University of Arkansas for Medical Sciences (UAMS), in accordance with the Guide for the Care and Use of Laboratory Animals (eighth edition) under protocol number 3405. Male Sprague-Dawley rats (Harlan Laboratories) were maintained in our Division of Laboratory Animal Medicine on a 12:12 light-to-dark cycle with free access to food and water.

At a weight of 250–290 grams, rats received local heart irradiation with the Small Animal Conformal Radiation Therapy Device developed at UAMS as described before [25] and in Supplementary Materials. The heart was exposed in 19 mm-diameter fields, one anterior-posterior and two lateral, at 3 Gy each (225 kV, 13 mA, 0.5 mm Cu-filtration resulting in 1.92 Gy/min at 1 cm tissue depth) to a total of 9 Gy per day for 5 consecutive days.

Sunitinib treatment

Oral administration of sunitinib (R&D Systems) or vehicle started on the first day of irradiation and continued once a day for 2 weeks. Two separate experiments were performed. Because the cardiac toxicity of radiation in combination with sunitinib was unknown, local heart irradiation was first combined with sunitinib at a relatively low dose of 8 mg/kg bodyweight per day. When no severe signs of toxicity were observed, a second experiment was performed with sunitinib at 15 mg/kg bodyweight per day. An oral dose of 15 mg/kg bodyweight is required for rats to reach sunitinib plasma levels comparable to those in patients at 24 hours after clinical doses of sunitinib [26]. Sunitinib was dissolved to 50 mg/ml in DMSO, diluted in saline, and a total volume of 500 μ l was administered by gavage. The rats were weighed every 2–3 days, and the ratio of sunitinib in DMSO and saline was adjusted every 6 days to correct for an increase in average rat weight. Each experiment contained 4 experimental groups: sham-irradiation + vehicle, sham-irradiation + sunitinib, 5x9 Gy + vehicle, and 5x9 Gy + sunitinib (5–6 animals per group). Every day, the vehicle group received oral DMSO and saline in the same ratio (total volume 500 μ l) as the sunitinib group.

Echocardiography

Echocardiography was performed as described before [27], using a Vevo 2100 imaging system (VisualSonics) with the MS250 transducer (13–24 MHz). Short axis M-mode recordings at the mid left ventricular (LV) level were used to obtain echocardiographic parameters.

Tissue and plasma preparation

At 2 weeks after local heart irradiation, rats were anesthetized with 3% isoflurane and injected i.v. with 100 U/kg heparin. Peripheral blood samples were collected into EDTA coated tubes and spun down to prepare plasma. The hearts were collected and cut longitudinally. One half, containing LV, right ventricle, and the interventricular septum, was placed in 10% formalin (8 mg/kg sunitinib experiment) or 5% formalin (15 mg/kg sunitinib experiment) for histological analysis. The remaining cardiac tissue was dissected to obtain

the LV, and a total of 180–200 mg was immediately used to isolate mitochondria. The remainder of the LV was divided and snap-frozen, to ensure that for each animal the glutathione analyses and Western-Blots described below were performed on cardiac tissue of the same anatomical location.

Ex vivo analysis of mitochondria

Isolation of mitochondria and measurements of mitochondrial permeability transition pore (mPTP) opening were performed as described before [28]. Freshly isolated mitochondria were resuspended in a swelling buffer and exposed to vehicle, 250 μM CaCl_2 , or 250 μM CaCl_2 in combination with the mPTP opening inhibitor cyclosporine A (CsA). MPTP opening in response to calcium leads to mitochondrial swelling as detected by a reduction in optical density at 540 nm (OD540). OD540 was measured with a Synergy 4 microplate reader (BioTek), immediately before the assay and every 2 minutes thereafter for a total of 20 minutes.

High-performance liquid chromatography quantification of glutathione

Approximately 50 mg of snap-frozen LV tissue was weighed and homogenized to evaluate levels of reduced glutathione (GSH) and oxidized glutathione (GSSG) by high-performance liquid chromatography (HPLC), as described before [29].

Western-Blots

Western-Blots were performed on LV tissue samples as described before [30;31]. Primary and HRP conjugated secondary antibodies are listed in Table 1S in the Supplementary Materials. Antibody binding was visualized with the Immobilon detection system (EMD Millipore) on CL-Xposure Film (Thermo Scientific). Films were scanned using an AlphaImager® gel documentation system (Protein Simple) and protein bands were quantified with ImageJ.

Histology

Apoptotic nuclei were detected in formalin-fixed tissue sections using the CardioTACS™ Kit (Trevigen), based on DNA end-labeling with terminal deoxynucleotidyl transferase. To stain for mast cells, sections were incubated in 0.5% Toluidine Blue in 0.5 N HCl for 72 hours, followed by 0.7 N HCl for 10 minutes. Apoptotic nuclei and mast cells in both ventricles were counted by an observer who was blinded to the treatment groups.

Collagen deposition was determined by incubating sections in Sirius Red (American MasterTech) supplemented with Fast Green (Fisher Scientific). Stained sections were scanned with a ScanScope CS2 slide scanner and analyzed with ImageScope 12 software (Aperio) to determine the percentage tissue area positive for collagens.

Electron microscopy

Tissue specimens of LV were fixed and processed for electron microscopy using a method described by Cocchiari et al [32]. Sections were analyzed with a Tecnai F20 200 keV electron microscope (FEI).

Cardiac troponin I

The concentration of cardiac troponin I (cTnI) in plasma samples was measured with a commercial ELISA kit (rat cTnI Ultra Sensitive, Life Diagnostics).

Mitochondrial membrane potential in cultured cardiomyocytes

Rat cardiomyocyte H9c2 cells (kindly provided by Nukhet Aykin-Burns) were used to determine mitochondrial membrane potential. H9c2 cells were maintained in DMEM (4.5 g/L D-glucose, 4.0 mM L-glutamine, 110 mg/L sodium pyruvate, 10% fetal bovine serum, Life Technologies) at 37°C in a 4% CO₂ incubator. Cells were irradiated using a ¹³⁷Cs source (Mark I model 68A, JL Shepherd, 5.1 Gy/min) at a dose of 9 Gy. Immediately after irradiation, 10 μM sunitinib or vehicle (DMSO) was added to the culture media, and cells were incubated at 37°C for 24 hours. Then, media were replaced with HBSS (1.4 mg/ml CaCl₂, 1 mg/ml MgCl₂) containing 10 μg/ml JC-1 (Life Technologies). The mitochondrial uncoupler carbonyl cyanide-4-(trifluoromethoxy) phenylhydrazone (FCCP, 50 μM, Sigma) was used as a positive control. After a 30-minute incubation in JC-1 +/- FCCP, cells were rinsed with HBSS and visualized with a fluorescence microscope (Axiovert 200M, Zeiss).

Statistical analysis

Data are presented as average ± standard error of the mean (sem). The two experiments (sunitinib at 8 and 15 mg/kg bodyweight) were analyzed separately. Ultrasound data were assessed with split-plot analysis of variance (ANOVA) with three fixed factors: radiation, sunitinib, and time (Proc GLM in SAS software), using Type III sums of squares with appropriately defined error terms [33]. All other data were analyzed with two-way ANOVA or repeated measures ANOVA (mitochondrial swelling assay), followed by Newman-Keuls individual comparisons (NCSS 8). A 5% significance level was set for main effects and interactions, with no adjustment for multiple testing.

Results

Echocardiography

Echocardiography was performed 1 week before and at 2 weeks after the start of radiation and sunitinib (15 mg/kg bodyweight per day). Because time alone had an effect on some parameters, we first determined whether there were significant interactions between the factors time and radiation, or time and sunitinib. Of the 15 parameters tested, 5 exhibited a significant sunitinib-by-time interaction. For all parameters, in the absence of sunitinib an increase was shown over time, and the increase was diminished by sunitinib (Figure 1S in Supplementary Materials, and Figure 1A). None of the parameters showed a significant radiation-by-time interaction. Finally, there was a significant sunitinib-by-radiation interaction in LV inner diameter and volume in systole. Here, radiation seemed to counteract the effects of sunitinib (Figure 1B). Ejection fraction is one of the main cardiac parameters that is altered by sunitinib in patients [18]. We observed no significant effects of radiation or sunitinib on ejection fraction in our rat model (Figure 2S in Supplementary Materials).

Cardiac cell death

Because tyrosine kinase pathways are involved in cardiomyocyte survival, TKI are sometimes thought to cause cardiac toxicity by inducing cell death. We therefore examined whether apoptosis had occurred. We discovered that the number of apoptotic nuclei detected was dependent on the tissue fixation, with higher numbers of positive nuclei in 5% compared to 10% formalin. We here show the results of the 5% formalin fixation (the 15 mg/kg bodyweight sunitinib experiment). Radiation caused an increase in number of apoptotic nuclei in interstitial cells (Figure 3S in Supplementary Materials), which was counteracted by sunitinib (Table 1).

Plasma cTnI

Plasma cTnI was measured as an indication of cardiac damage (Table 1). Local heart irradiation caused an increase in plasma cTnI, which was not modified by sunitinib.

Cardiac remodeling

We previously observed that cardiac mast cell numbers are significantly reduced up to 1 month after local heart irradiation [34]. While sunitinib alone did not modify cardiac mast cell numbers, at both dose levels there was a non-significant trend towards an exacerbation of the effects of radiation (Table 1). We found no significant changes in LV collagen deposition in any of the treatment groups (data not shown).

Oxidative stress

Radiation caused a significant reduction in LV GSH levels, leading to a decrease in GSH/GSSG, together with an increase in protein 4-hydroxynonenal (4-HNE) adducts (Figure 4S and 5S in Supplementary Materials). Sunitinib caused similar alterations, especially at the higher dose, but did not potentiate the effects of radiation. Radiation caused an increase in LV expression of glutathione peroxidase 1/2 (GPX-1/2), superoxide dismutase 2 (SOD2), peroxiredoxin 5 (PRX5), and heme oxygenase 1 (HO-1). Sunitinib inhibited the effects of radiation on GPX-1/2 and SOD2, but enhanced the effects on PRX5 and HO-1 (Figure 6S in Supplementary Materials).

Mitochondrial alterations

Electron microscopy was performed after sunitinib at 15 mg/kg bodyweight per day (Figure 2). Mitochondria with concentric cristae were observed in irradiated hearts. Sunitinib caused a different pattern of mitochondrial damage dominated by disorganized and thinning cristae. Mitochondrial damage seemed most severe in the combined treatment group. In addition, disorganization of myofibrils was observed, most prominently after sunitinib.

We performed a swelling assay with isolated mitochondria to determine their tendency towards mPTP opening. *Ex vivo* incubation with calcium induced mPTP opening in mitochondria isolated from irradiated hearts. Sunitinib caused the same effects as local heart irradiation. Moreover, when administered at a dose of 15 mg/kg/bodyweight per day, sunitinib potentiated the effects of local heart irradiation (Figure 3).

Rat cardiomyocytes were used to identify the effects of radiation and sunitinib on mitochondrial membrane potential (Figure 7S in Supplementary Materials). JC-1 taken up in vehicle treated, sunitinib treated, and irradiated H9c2 cells was mostly red fluorescent, indicating that these cells had mitochondria with a normal membrane potential. Radiation in combination with sunitinib increased green fluorescence, suggesting that the two treatments combined caused a reduction in the mitochondrial membrane potential.

Discussion

This study examined the effects of local heart irradiation combined with 2 weeks of sunitinib treatment on cardiac function and structure in a rat model. While sunitinib alone had some effects on echocardiographic parameters, most effects on cardiac function seemed diminished in the combined treatment group. The apparent antagonistic effects of radiation and sunitinib on cardiac function are interesting and deserve further investigation. On the other hand, sunitinib enhanced the effects of radiation on mitochondrial morphology and swelling. An increase in plasma cTnI may only occur after higher doses of sunitinib [35].

Local heart irradiation in our rat model causes an increase in the number of apoptotic nuclei at time points up to 2 weeks [36]. While the exact nature of the apoptotic nuclei is unclear, their appearance suggests that they are not of cardiomyocytes. Instead, interstitial cells such as fibroblasts or infiltrating inflammatory cells may have undergone apoptosis in response to radiation. This could have possibly been in response to a secondary signals as part of an active process of cell removal [37]. Sunitinib alone did not induce an increase in apoptotic nuclei. Moreover, sunitinib counteracted the effects of radiation. Hence, apoptotic cell death may not be the main mechanism of cardiac toxicity from sunitinib.

Cardiomyocytes carry large numbers of mitochondria and are highly dependent on them for survival. We observed severe changes in mitochondrial morphology after irradiation and sunitinib treatment *in vivo* and a reduced mitochondrial membrane potential when radiation and sunitinib were combined *in vitro*. However, because of differences in model characteristics and follow-up times, the *in vivo* and *in vitro* results must be compared with caution. Alterations in mitochondrial membrane properties have been observed in other animal models of sunitinib treatment [22] and local heart irradiation [38], and mitochondria isolated from the irradiated rat heart are more prone to mPTP opening as observed within hours up to several months after irradiation [36]. Here, radiation and sunitinib combined had the most severe effect on mPTP opening. On the other hand, while radiation and sunitinib both caused indications of cardiac oxidative stress, they did not potentiate each other. The mitochondrial parameters included in the current study are no indication of mitochondrial function. Additional studies are required to determine the role of mitochondria in cardiac effects of radiation and sunitinib.

In our rat model, increased collagen deposition in the heart occurs at about 3 months after irradiation and gets progressively worse after that. Together with tissue degeneration and fibrosis, electrophysiological disturbances are observed, such as those indicative of a third-degree heart block [30]. Because of the early time point in this study, radiation-induced fibrosis or conduction abnormalities were not observed. Sunitinib did not cause fibrosis

either, alone or in combination with radiation. Indeed, TKI do not always aggravate cardiac remodeling. For instance, lapatinib did not modify radiation-induced cardiac toxicity in a mouse model [39]. Moreover, sunitinib reduced right ventricular remodeling in pulmonary hypertension [40]. Since radiation is known to cause late cardiac fibrosis, the long-term effects of radiation and sunitinib still need to be investigated.

In our rat model, cardiac mast cell numbers are significantly reduced within 1 month after local heart irradiation, followed by a time-dependent increase that coincides with collagen deposition [34]. Sunitinib inhibits several tyrosine kinases involved in mast cell development, survival, and proliferation [41]. Because the effects of radiation alone on cardiac mast cell number was strong, a further reduction of mast cell numbers by sunitinib was not statistically significant.

While the cardiac effects of localized irradiation are likely due to a direct effect on the heart, TKIs have effects on other organs, such as the liver [42], which may affect the heart. Also, sunitinib may modify the vasculature by inhibiting vascular endothelial growth factor receptors, or by altering pericyte function via inhibition of platelet derived growth factor receptors [22]. Because of the relative newness of TKIs, the number of reported studies into mechanisms by which they may cause cardiac toxicity is still somewhat limited.

In conclusion, this preclinical study suggests that cardiac radiation exposure combined with sunitinib treatment may not cause severe acute toxicity. Long-term effects remain to be determined.

Supplementary Material

Refer to Web version on PubMed Central for supplementary material.

Acknowledgments

This work was supported by NIH/NCI (CA148679), NIH/NIGMS (P20 GM109005), and the American Cancer Society (RSG-10-125-01-CCE). The electron microscopy was performed by the UAMS Digital Microscopy Core that is supported by NIH (UL1TR000039). The authors thank Ralph Kodell for his expert advice on statistical analyses.

Role of the Funding Sources

The study sponsors had no role in the study design, collection, analysis, interpretation of the data, or in the writing of the manuscript.

References

1. Adams MJ, Hardenbergh PH, Constine LS, Lipshultz SE. Radiation-associated cardiovascular disease. *Crit Rev Oncol Hematol*. 2003; 45:55–75. [PubMed: 12482572]
2. Gatta G, Zigon G, Capocaccia R, et al. Survival of European children and young adults with cancer diagnosed 1995–2002. *Eur J Cancer*. 2009; 45:992–1005. [PubMed: 19231160]
3. Heidenreich PA, Hancock SL, Vagelos RH, Lee BK, Schnittger I. Diastolic dysfunction after mediastinal irradiation. *Am Heart J*. 2005; 150:977–82. [PubMed: 16290974]
4. Kole TP, Aghayere O, Kwah J, Yorke ED, Goodman KA. Comparison of Heart and Coronary Artery Doses Associated with Intensity-Modulated Radiotherapy Versus Three-Dimensional Conformal

- Radiotherapy for Distal Esophageal Cancer. *Int J Radiat Oncol Biol Phys.* 2012; 83:1580–6. [PubMed: 22284687]
5. Tillman GF, Pawlicki T, Koong AC, Goodman KA. Preoperative versus postoperative radiotherapy for locally advanced gastroesophageal junction and proximal gastric cancers: a comparison of normal tissue radiation doses. *Dis Esophagus.* 2008; 21:437–44. [PubMed: 19125798]
 6. Wu WC, Chan CL, Wong YW, Cuijpers JP. A study on the influence of breathing phases in intensity-modulated radiotherapy of lung tumours using four-dimensional CT. *Br J Radiol.* 2009; 83:252–6. [PubMed: 19723769]
 7. Fabian MA, Biggs WH III, Treiber DK, et al. A small molecule-kinase interaction map for clinical kinase inhibitors. *Nat Biotechnol.* 2005; 23(3):329–36. [PubMed: 15711537]
 8. Halmos B, Jia Y, Bokar JA, et al. A Phase I Study of the combination of oxaliplatin/docetaxel and vandetanib for the treatment of advanced gastroesophageal cancer. *Invest New Drugs.* 2013; 31:1244–50. [PubMed: 23553066]
 9. Reynolds C, Spira AI, Gluck L, et al. Sunitinib malate in previously untreated, nonsquamous, non-small cell lung cancer patients over the age of 70 years: Results of a Phase II trial. *Invest New Drugs.* 2013; 31:1330–8. [PubMed: 23761052]
 10. Groen HJ, Socinski MA, Grossi F, et al. A randomized, double-blind, phase II study of erlotinib with or without sunitinib for the second-line treatment of metastatic non-small-cell lung cancer (NSCLC). *Ann Oncol.* 2013; 24:2382–9. [PubMed: 23788751]
 11. Murphy CG, Morris PG. Recent advances in novel targeted therapies for HER2-positive breast cancer. *Anticancer Drugs.* 2012; 23:765–76. [PubMed: 22824822]
 12. Bamias A, Tzannis K, Beuselinck B, et al. Development and validation of a prognostic model in patients with metastatic renal cell carcinoma treated with sunitinib: a European collaboration. *Br J Cancer.* 2013; 109:332–41. [PubMed: 23807171]
 13. Crown JP, Dieras V, Staroslawska E, et al. Phase III Trial of Sunitinib in Combination With Capecitabine Versus Capecitabine Monotherapy for the Treatment of Patients With Pretreated Metastatic Breast Cancer. *J Clin Oncol.* 2013; 31:2870–8. [PubMed: 23857972]
 14. Rugo HS, Stopeck AT, Joy AA, et al. Randomized, placebo-controlled, double-blind, phase II study of axitinib plus docetaxel versus docetaxel plus placebo in patients with metastatic breast cancer. *J Clin Oncol.* 2011; 29:2459–65. [PubMed: 21555686]
 15. Twardowski PW, Beumer JH, Chen CS, et al. A phase II trial of dasatinib in patients with metastatic castration-resistant prostate cancer treated previously with chemotherapy. *Anticancer Drugs.* 2013; 24:743–53. [PubMed: 23652277]
 16. Schutz FA, Je Y, Richards CJ, et al. Meta-analysis of randomized controlled trials for the incidence and risk of treatment-related mortality in patients with cancer treated with vascular endothelial growth factor tyrosine kinase inhibitors. *J Clin Oncol.* 2012; 30:871–7. [PubMed: 22312105]
 17. Reichardt P, Kang YK, Rutkowski P, et al. Clinical outcomes of patients with advanced gastrointestinal stromal tumors: safety and efficacy in a worldwide treatment-use trial of sunitinib. *Cancer.* 2015; 121:1405–13. [PubMed: 25641662]
 18. Di Lorenzo G, Autorino R, Bruni G, et al. Cardiovascular toxicity following sunitinib therapy in metastatic renal cell carcinoma: a multicenter analysis. *Ann Oncol.* 2009; 20:1535–42. [PubMed: 19474115]
 19. Magne N, Chargari C, MacDermid D, et al. Tomorrow's targeted therapies in breast cancer patients: what is the risk for increased radiation-induced cardiac toxicity? *Crit Rev Oncol Hematol.* 2010; 76:186–95. [PubMed: 20138541]
 20. Witteles RM, Telli M. Underestimating cardiac toxicity in cancer trials: lessons learned? *J Clin Oncol.* 2012; 30:1916–18. [PubMed: 22454419]
 21. O'Farrell AM, Abrams TJ, Yuen HA, et al. SU11248 is a novel FLT3 tyrosine kinase inhibitor with potent activity in vitro and in vivo. *Blood.* 2003; 101:3597–605. [PubMed: 12531805]
 22. Chintalgattu V, Rees ML, Culver JC, et al. Coronary microvascular pericytes are the cellular target of sunitinib malate-induced cardiotoxicity. *Sci Transl Med.* 2013; 5:187ra69.
 23. Blasi E, Heyen J, Patyna S, et al. Sunitinib, a receptor tyrosine kinase inhibitor, increases blood pressure in rats without associated changes in cardiac structure and function. *Cardiovasc Ther.* 2012; 30:287–94. [PubMed: 21884012]

24. Kerkela R, Woulfe KC, Durand JB, et al. Sunitinib-induced cardiotoxicity is mediated by off-target inhibition of AMP-activated protein kinase. *Clin Transl Sci.* 2009; 2:15–25. [PubMed: 20376335]
25. Sharma S, Moros EG, Boerma M, et al. A novel technique for image-guided local heart irradiation in the rat. *TCRT Express.* 2013; 1:47–57.
26. Speed B, Bu HZ, Pool WF, et al. Pharmacokinetics, distribution, and metabolism of [14C]sunitinib in rats, monkeys, and humans. *Drug Metab Dispos.* 2012; 40:539–55. [PubMed: 22180047]
27. Sridharan V, Tripathi P, Sharma SK, et al. Cardiac inflammation after local irradiation is influenced by the kallikrein-kinin system. *Cancer Res.* 2012; 72:4984–92. [PubMed: 22865451]
28. Sridharan V, Aykin-Burns N, Tripathi P, et al. Radiation-induced alterations in mitochondria of the rat heart. *Radiat Res.* 2014; 181(3):324–34. [PubMed: 24568130]
29. Sridharan V, Tripathi P, Aykin-Burns N, et al. A tocotrienol-enriched formulation protects against radiation-induced changes in cardiac mitochondria without modifying late cardiac function or structure. *Radiat Res.* 2015; 183:357–66. [PubMed: 25710576]
30. Sridharan V, Tripathi P, Sharma S, et al. Effects of late administration of pentoxifylline and tocotrienols in an image-guided rat model of localized heart irradiation. *PLoS One.* 2013; 8:e68762. [PubMed: 23894340]
31. Sridharan V, Tripathi P, Sharma S, et al. Roles of sensory nerves in the regulation of radiation-induced structural and functional changes in the heart. *Int J Radiat Oncol Biol Phys.* 2014; 88:167–74. [PubMed: 24331664]
32. Cocchiari JL, Kumar Y, Fischer ER, Hackstadt T, Valdivia RH. Cytoplasmic lipid droplets are translocated into the lumen of the Chlamydia trachomatis parasitophorous vacuole. *Proc Natl Acad Sci U S A.* 2008; 105:9379–84. [PubMed: 18591669]
33. Winer, BJ.; Brown, DR.; Michels, KM. *Statistical Principles in Experimental Design.* 3. New York City: McGraw-Hill; 1991.
34. Boerma M, Zurcher C, Esveldt I, Schutte-Bart CI, Wondergem J. Histopathology of ventricles, coronary arteries and mast cell accumulation in transverse and longitudinal sections of the rat heart after irradiation. *Oncol Rep.* 2004; 12:213–9. [PubMed: 15254680]
35. Bordun KA, Premecz S, daSilva M, et al. The utility of cardiac biomarkers and echocardiography for the early detection of bevacizumab- and sunitinib-mediated cardiotoxicity. *Am J Physiol Heart Circ Physiol.* 2015; 309:H692–H701. [PubMed: 26092985]
36. Sridharan V, Aykin-Burns N, Tripathi P, et al. Radiation-induced alterations in mitochondria of the rat heart. *Radiat Res.* 2014; 181:324–34. [PubMed: 24568130]
37. Fox S, Leitch AE, Duffin R, Haslett C, Rossi AG. Neutrophil apoptosis: relevance to the innate immune response and inflammatory disease. *J Innate Immun.* 2010; 2:216–27. [PubMed: 20375550]
38. Cilliers GD, Harper IS, Lochner A. Radiation-induced changes in the ultrastructure and mechanical function of the rat heart. *Radiother Oncol.* 1989; 16:311–26. [PubMed: 2616818]
39. Seemann I, te Poele JA, Song JY, Hoving S, Russell NS, Stewart FA. Radiation- and anthracycline-induced cardiac toxicity and the influence of ErbB2 blocking agents. *Breast Cancer Res Treat.* 2013; 141:385–95. [PubMed: 24091769]
40. Kojonazarov B, Sydykov A, Pullamsetti SS, et al. Effects of multikinase inhibitors on pressure overload-induced right ventricular remodeling. *Int J Cardiol.* 2013; 167:2630–7. [PubMed: 22854298]
41. Ferguson MJ, Rhodes SD, Jiang L, et al. Preclinical Evidence for the Use of Sunitinib Malate in the Treatment of Plexiform Neurofibromas. *Pediatr Blood Cancer.* 2016; 63:206–13. [PubMed: 26375012]
42. Ghatalia P, Je Y, Mouallem NE, et al. Hepatotoxicity with vascular endothelial growth factor receptor tyrosine kinase inhibitors: A meta-analysis of randomized clinical trials. *Crit Rev Oncol Hematol.* 2015; 93:257–76. [PubMed: 25523486]

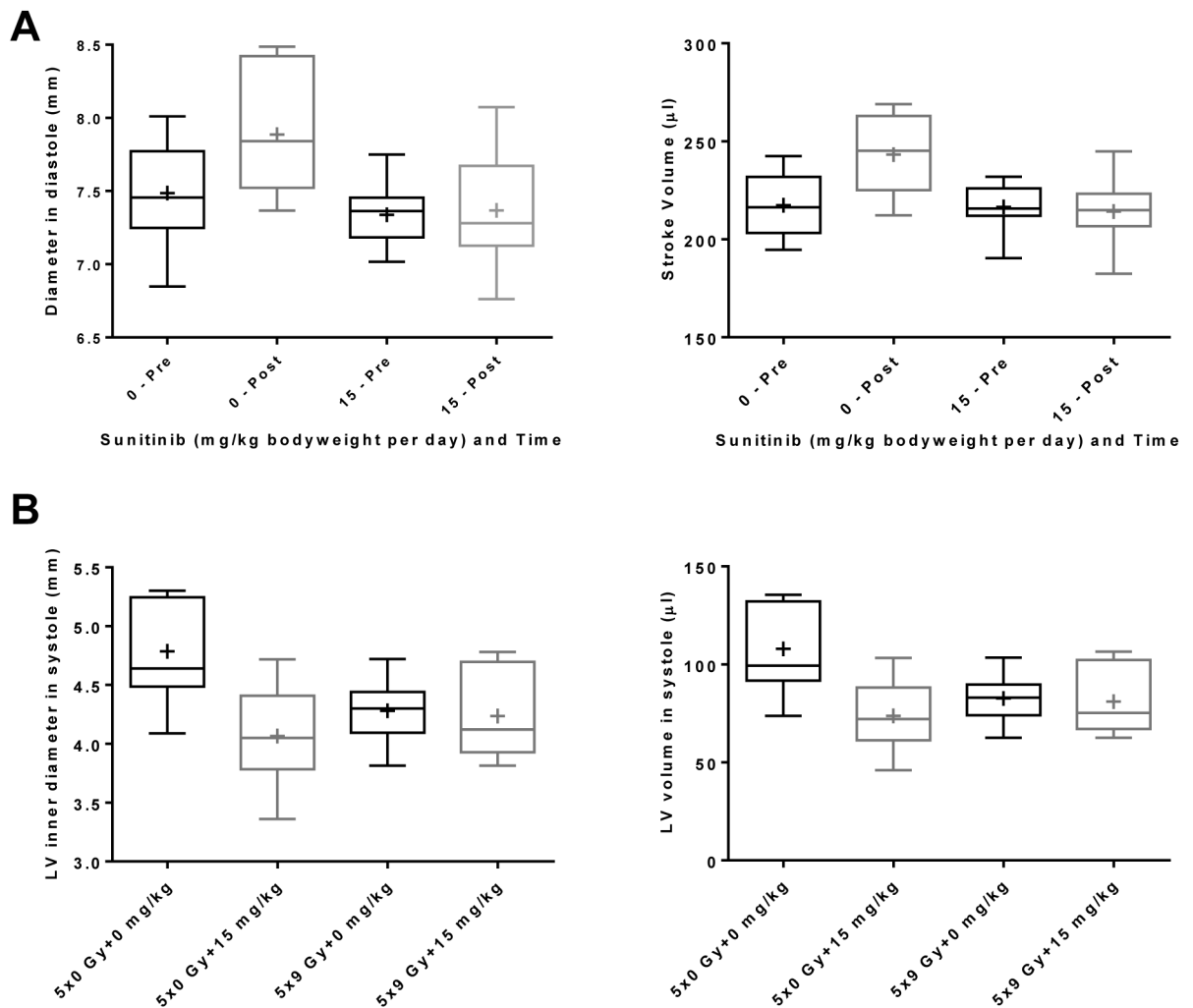


Figure 1. Effects of local heart irradiation and sunitinib on echocardiography parameters
A) Box plots of two of the M-mode parameters that showed a significant interaction between sunitinib and time: Diameter in diastole ($p=0.02$) and Stroke Volume ($p=0.0001$). Box plots of all five parameters with a significant interaction between sunitinib and time are shown in Figure 1S in Supplementary Materials. **B)** Box plots of the two M-mode parameters that showed a significant interaction between radiation and sunitinib: LV inner diameter in systole ($p=0.02$) and LV volume in systole ($p=0.02$). Box: 25th – 75th percentiles, whiskers: minimum – maximum, horizontal line: median, +: average, $n=10$.

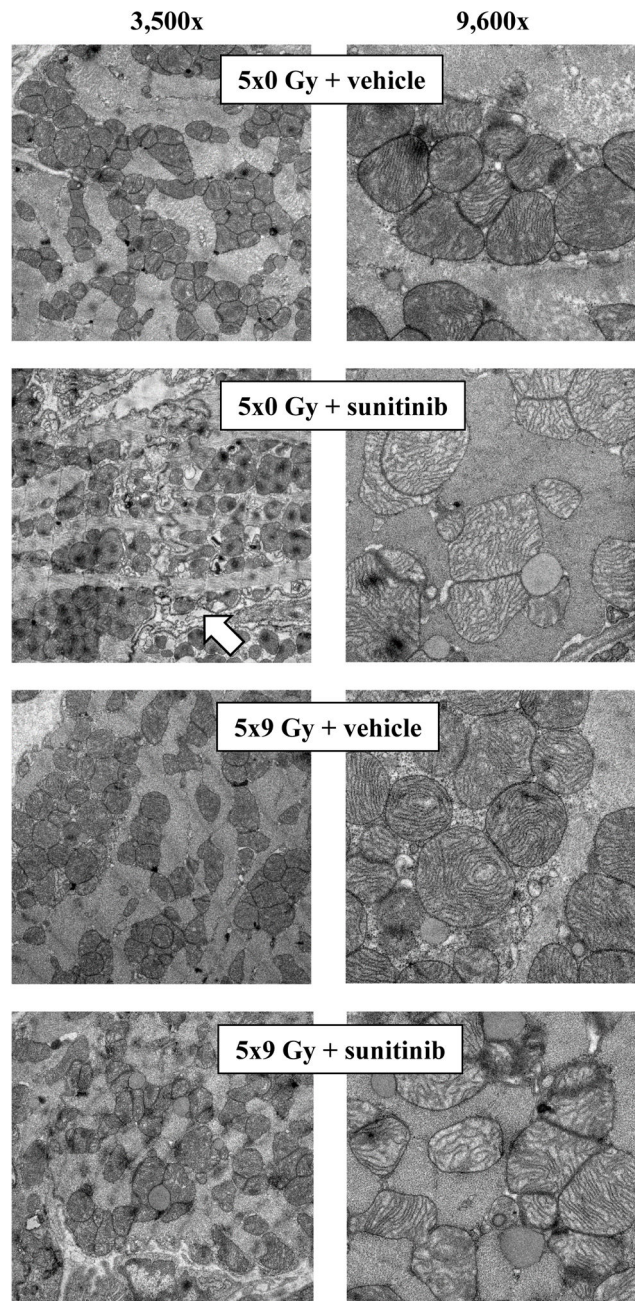


Figure 2. Effects of local heart irradiation and sunitinib on mitochondrial morphology
Electron microscopy was performed after local heart irradiation and sunitinib at 15 mg/kg bodyweight per day. Images at magnification 3,500 \times reveal disorganization of myofibrils in the sunitinib treatment group (arrow).

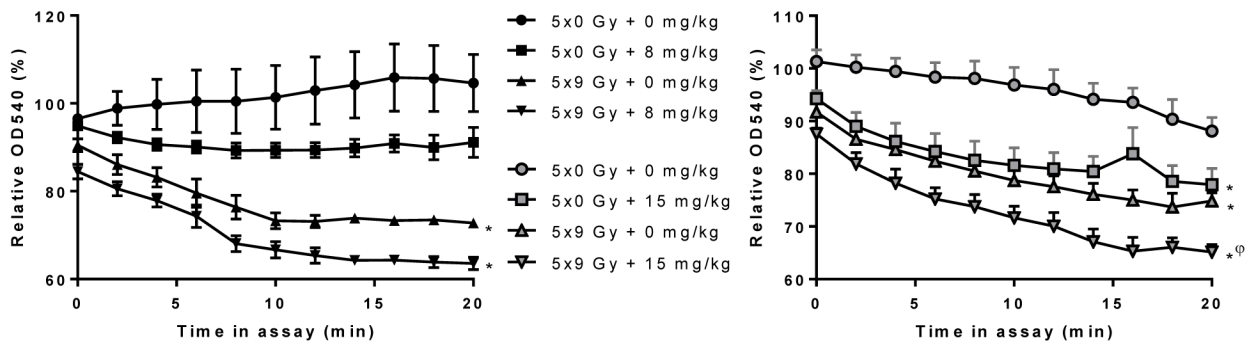


Figure 3. Effects of local heart irradiation and sunitinib on the tendency for mitochondria to swell

The graphs indicate the OD540 of isolated mitochondria when in the swelling assay, relative to OD540 of each sample immediately before the assay. Incubation of mitochondria with CaCl₂ + CsA, or no CaCl₂ caused no swelling (data not shown). Average \pm sem (n=4–5).

*p<0.05 vs. sham + vehicle; Φ p<0.05 vs. sham + sunitinib.

Table 1

Effects of local heart irradiation and sunitinib on cardiac apoptosis, cardiac mast cell numbers, and plasma cTnI. Average \pm sem (n=5–6).

Experimental group	Number of apoptotic nuclei	Number of mast cells	Plasma cTnI (ng/ml)
Experiment 1: sunitinib at 8 mg/kg bodyweight per day			
5x0 Gy + vehicle	ND	210 \pm 14	0.08 \pm 0.004
5x0 Gy + sunitinib	ND	203 \pm 41	0.09 \pm 0.003
5x9 Gy + vehicle	ND	22 \pm 6 ^{*#}	0.12 \pm 0.001 ^{*#}
5x9 Gy + sunitinib	ND	11 \pm 3 ^{*#}	0.13 \pm 0.004 ^{*#}
Experiment 2: sunitinib at 15 mg/kg bodyweight per day			
5x0 Gy + vehicle	827 \pm 61	182 \pm 13	0.08 \pm 0.002
5x0 Gy + sunitinib	904 \pm 97	155 \pm 20	0.09 \pm 0.001
5x9 Gy + vehicle	1631 \pm 97 ^{*#}	20 \pm 3 ^{*#}	0.13 \pm 0.002 ^{*#}
5x9 Gy + sunitinib	1053 \pm 70 [†]	4 \pm 1 ^{*#}	0.14 \pm 0.007 ^{*#}

ND: not determined.

* p<0.05 vs. sham + vehicle;

p<0.05 vs. sham + sunitinib.

† p<0.05 vs. radiation + vehicle